

**SYSTEMATIC DEPENDENCE OF THE
OPTICAL SECOND HARMONIC GENERATION INTENSITY
ON THE DESIGNED PARAMETERS OF Cr NANOHOLES**

**Ngo Khoa Quang^{1,*}, Yoshihiro Miyauchi², Goro Mizutani³, Martin D.Charlton⁴,
Ruiqi Chen⁴, Stuart Boden⁴ and Harvey Rutt⁴**

¹*Hue College of Science, Hue University, 77 Nguyen Hue, Hue, Vietnam*

²*Department of Applied Physics, National Defense Academy,
Hashirimizu 1-10-20, Yokosuka-shi, Kanagawa 239-8686, Japan*

³*School of Materials Science, Japan Advanced Institute of Science and Technology,
1-1 Asahidai, Nomi, Ishikawa 923-1292, Japan*

⁴*School of Electronics and Computer Science, University of Southampton, SO17 1BJ, UK*

*E-mail: khoaquang@gmail.com

Abstract. We observed the optical second harmonic generation (SHG) from the arrays of V-shaped chromium nanoholes fabricated by electron beam lithography. To consider the dependence of the SHG response on the structural parameters of apex angles (A) and arm lengths (L) of V shaped Cr nanoholes, we performed azimuthal measurement Pin/Pout configuration for the V-shaped subwavelength nanoholes. Three sets of the V shape with A of 60° , 90° and 120° show enhancement in SHG intensity when L increases. We discussed the possible sources of the obtained SHG signal difference. We proposed that the obtained SHG signal should result from the bulk contribution.

Keywords: *Second harmonic generation (SHG); Cr metal; Nanoholes.*

I. INTRODUCTION

Metamaterials have many fascinating features [1]. By designing the deliberated geometries, one can utilize the surprising behaviors of nanostructures such as negative refractive index [2], local field enhancement [3], or plasmon excitation [4]. From second order optical standpoint, the recent reports researched on the second order optical effects have emphasized that metal materials give rise to a very complicated state, especially at nanoscale [5, 6]. Both surface (electric dipole) and bulk (magnetic dipole and electric quadrupole) contributions can appear equally in the second harmonic generation (SHG) magnitude whereas the surface term is usually considered as feasible candidate [7]. Hence, clarifying the role of the local surface and nonlocal bulk contribution becomes particularly necessary to control and optimize the nonlinear optical behavior of the metallic nanostructures for the functional applications.

In this study, we investigated the nonlinear susceptibility properties of V-shaped subwavelength slits formed in a 15-nm-thick chromium. Three sets of the V-shaped nanoholes were fabricated. We measured the azimuthal angular dependence of the SHG from the sample and their SHG intensities were compared with each other. We attempted to examine the dependence of the SHG response on the structural parameters of V-shaped

chromium nanoholes. The work is therefore expected to provide new information in adjustment of the nonlinear optical behavior of metamaterial for relevant applications.

II. EXPERIMENT

The silica substrate was first coated with 15 nm Cr by evaporation. The sample was then spin-coated with a 40 nm e-beam resist and patterned by e-beam lithography. After resist development, the patterns were then transferred to Cr using dry etch processes before removing the resist completely. The design parameters of the V-shaped apertures are depicted in Fig. 1(a). The apex angle A was set either as 60° , 90° or 120° . The arm width W was 50 nm. For each value of A , we fabricated nanoholes with arm lengths $L = 2W$, $3W$ and $4W$. All the arrays were created in the same batch to minimize the variation of the condition in the fabrication process. Atomic force microscopy images of the fabricated structures are shown in Figs. 1(b)-1(j).

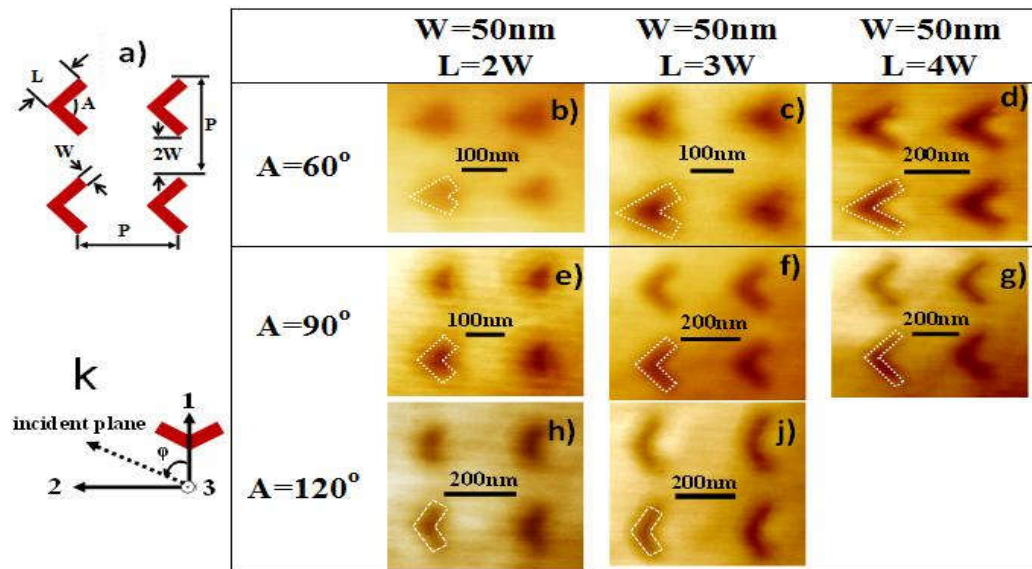


Fig. 1. Structure of V-shaped subwavelength nanohole array: (a) scheme of the designed parameters and atomic force microscopy image of the first set (b-d) of V-shaped arrays with 60° apex angle, the second set (e-g) of V-shaped arrays with 90° apex angle, and the third set (h-j) of V-shaped arrays with 120° apex angle. The dotted line shows the designed “V”-shapes.

As the excitation source of the SHG signal from the sample, I used the second harmonic denoted ω of a mode-locked Nd:YAG picosecond laser. Its output pulse width was 30 ps and the repetition rate was 10Hz. For measuring the azimuthal angle dependence of the SHG, the sample was mounted on an automatic rotation stage. The incident polarized light at the photon energy of 2.33 eV illuminated the V-shaped area at an angle of 45° with respect to the surface normal. Direction 3 is defined as the direction normal to the surface while directions 1 and 2 are on the sample surface. 1 indicates the direction of the bisector of the V passing through its apex in the substrate plane. Azimuthal angle ϕ is defined as the angle between the incident plane and direction 1. At 0° , the fundamental

light first illuminates the nanohole arrays at the valley between the two arms of the V-shaped structure. Fig. 1(k) illustrates the relative position between the incident plane and direction 1.

III. RESULTS AND DISCUSSION

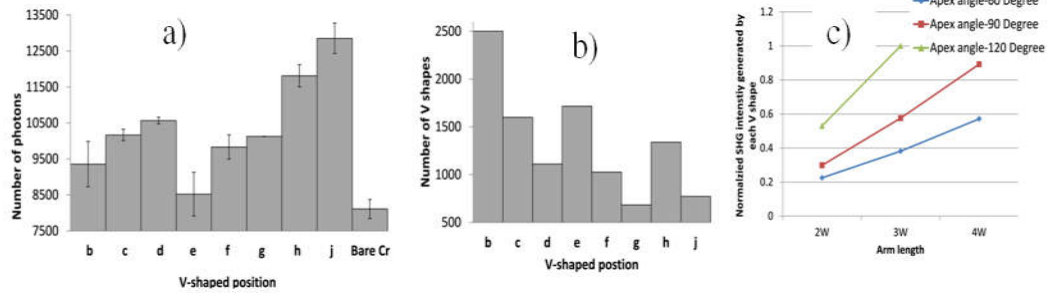


Fig. 2. (a) The summation of the consecutive SHG intensity of V-shaped nanohole arrays and bare chromium substrate from 0° to 350° in Pin/Pout configuration. The character under each bar corresponds to the V-shaped array indicated in Figs. 5.3(b)-5.3(j). (b) Number of V shaped nanoholes in each array. (c) The normalized SHG intensity emitted from each V shape calculated by dividing the total SHG intensity in (a) by the total V shaped nanoholes in (b).

To consider the dependence of the SHG response on the structural parameters of V-shaped chromium nanoholes, we performed azimuthal measurement of all arrays shown in Figs. 1(b)-1(j) in the same experiment condition. As a control, the SHG signal from a bare Cr substrate was measured. The experimental data of each array were then added consecutively from 0° to 350° to make the comparison. The numbers of SHG photons in Pin/Pout configuration of all arrays are presented in Fig. 2(a). The character under each bar corresponds to the V-shaped array indicated in Figs. 1(b)-1(j). We estimated tentatively the contribution of individual V shape by dividing the total SHG intensity in Fig. 3(a) by the corresponding total numbers of V shaped nanoholes in Fig. 3(b). The result is shown in Fig. 3(c).

We discuss the possible sources of the obtained SHG signal difference shown in Fig. 3(c). The plasmon excitation did not emerge in previous report [8], therefore the obtained SHG signal should result from nonlinear susceptibility elements $\chi_{313}^{(2)}$ of V-shaped nanoholes, resulting from the bulk contribution. Second order nonlinear polarization in nanostructure can be expressed as a generalized polarization [9]:

$$P(2\omega) = P - \nabla \cdot Q + \frac{\mu_0}{i\omega} \nabla \times M + \dots \quad (1)$$

The second and the third terms can be rewritten in an isotropic medium as,

$$P_3^{bulk}(2\omega) \propto \Gamma_{3311} E_3(\omega) \nabla_1 E_1(\omega) + \Gamma_{3113} E_1(\omega) \nabla_1 E_3(\omega) \quad (2)$$

Here, Γ_{ijkl} is the third rank susceptibility tensor, and $E_j(\omega)$ and $E_i(\omega)$ are the two applied electric fields at frequency ω . The two terms in Eq. (2) give effectively the second order response to the electric field. There are vertical metallic sidewalls contained within each V-shaped hole and they have air-chromium metal boundaries [8]. This has a strong effect on the gradient operator ∇_1 shown in Eq. (2).

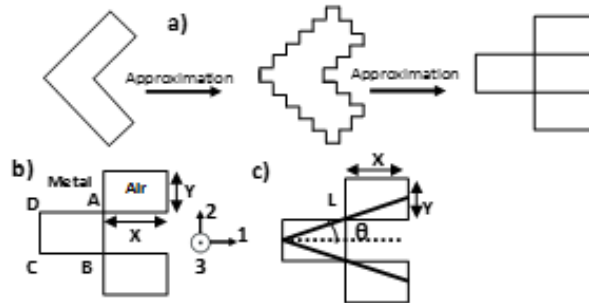


Fig. 3. Three rectangular holes formed in Cr metal could tentatively form a model of V-shaped hole structure: (a) Two-step approximation of a V-shaped hole by three rectangular holes; (b) initial and (c) final position of rectangular holes after rotating 180°. (d) Definition of θ .

Tentatively, three rectangular holes formed in Cr metal as depicted in Fig. 3(b) could make a model of V-shaped hole structure based on the process of approximation in Fig. 3(a). Here, the analysis methodology used is quite similar to that used in finite-difference time-domain method. By doing the same calculation as explained in Ref. [10], the total nonlinear polarization created by this rectangular hole is,

$$P_3^{total}(2\omega) \propto -(1/2t)E_1(\omega)E_3(\omega)(\Gamma_{3311} + \Gamma_{3113})k_1^2 X^2 Y \quad (3)$$

We introduce the factor 1/t because, in principle, the rate of field gradient has to be inversely proportional to length of scope t and k_1 is the wave vector. We now try to interpret the effect of the arm length as well as the apex angle, by investigating Eq. (3) and Fig. 3(b). Here, increasing the arm length corresponds to increasing X and Y values in the same rate. Making a larger apex with constant arm length L means increasing the Y and decreasing the X values at the same time. According to Eq. (3), $P_3^{total}(2\omega)$ increases as X and Y increases. In Fig. 3(c), the SHG intensity increases as the arm length L is increased and it is consistent with this prediction.

Using the angle θ , a half of apex angle A seen in the simple model shown in Fig. 3(c), the X and Y values are expressed as $X = (1/2)L \cos \theta$ and $Y = L \sin \theta$, respectively. Then, the nonlinear polarization has the form,

$$P_3^{total}(2\omega) \propto (1/4)L^3 \sin \theta \cos^2 \theta \quad (4)$$

$(1/4)L^3 \sin \theta \cos^2 \theta$ in Eq. (4) is numerically calculated as $\sim 0.094L^3$ at $\theta = 30^\circ$, $\sim 0.088L^3$ at $\theta = 45^\circ$, and $\sim 0.054L^3$ at $\theta = 60^\circ$. The result obtained in Fig. 2 (c), however, indicated that SHG intensity increased together with the enlargement of the apex angle. The

discrepancy between the model and the experimental data might result from the complexity of the other parameters not incorporated into this simple model. In addition, in Fig. 1 the shapes of the nanoholes are more obscure when the apex angle A has small angle. Since the shapes are less perfect, the SHG intensity is reduced consequently.

IV. CONCLUSION

In this research, we have shown that there is a systematic dependence of the SHG intensity on the designed parameters of Cr nanoholes, especially on the arm length. Simple model was given and its limit was also clarified. In particular, the strong field gradient at the boundaries of the holes gives rise to the nonlinear response. For favorable material exploited for artificial nanostructures such as gold, plasmon excitation enhancing nonlinear optical effect could be accomplished. However, in the case of Cr metal plasmon was silent and the nonlinear optical behavior results from the bulk contribution of Cr electrons. This can be useful for designing artificial nonlinear optical materials with different properties from those made of plasmonic materials.

REFERENCES

- [1] M. Kauranen, and A. V. Zayats, *Nat. Photonics*. Vol. **6**, 2012, pp. 737–748.
- [2] W. Cai, U. K. Chettiar, A. V. Kildishev, and V. M. Shalaev, *Nat. Photonics*. Vol. **1**, 2007, pp. 224 - 227.
- [3] A. Lesuffleur, L. K. S. Kumar, and R. Gordon, *Phys. Rev. B*. Vol. **75**, 2007, pp. 045423–045427.
- [4] C. Hubert, L. Billot, P. M. Adam, R. Bachelot, and P. Royer, *Appl. Phys. Lett.* Vol. **90**, 2007, pp. 181105–181107.
- [5] Y. R. Shen, *Appl. Phys. B*. Vol. **68**, 1999, pp. 295-300.
- [6] F. X. Wang, F. J. Rodríguez, W. M. Albers, R. Ahorinta, J. E. Sipe, and M. Kauranen, *Phys. Rev. B*. Vol. **80**, 2009, pp. 233402(1-4).
- [7] M. Zdanowicz, S. Kujala, and H. Husu, *New J. Phys.* Vol. **13**, 2011, pp. 023025 (1-11).
- [8] N. K. Quang, Y. Miyauchi, G. Mizutani, M. D. Charlton, R. Chen, S. Boden, H. Rutt, *Jpn. J. Appl. Phys.* Vol. **53**, 2014, pp. 02BC11(1-5).
- [9] P. F. Brevet, *Surface Second Harmonic Generation*, Presses Polytechniques Universitaires Romandes, Lausanne, 1997.
- [10] N. K. Quang, Y. Miyauchi, G. Mizutani, M. D. Charlton, R. Chen, S. Boden, H. Rutt, *Surf. Interface Anal.* Vol. **46**, 2014, pp. 1119–1300.